Fibers and Polymers 2021, Vol.22, No.1, 87-96
DOI 10.1007/s12221-021-9049-6

ISSN 1229-9197 (print version)
ISSN 1875-0052 (electronic version)

The Effect of Silver Concentration on Ag-TiO_2 Nanoparticles Coated Polyester/Cellulose Fabric by In situ and Ex situ Photo-reduction Method – A Comparative Study

Zahra Moridi Mahdieh[1,2], Shahla Shekarriz[1,2]*, and Faramarz Afshar Taromi[1]

[1]*Department of Polymer Engineering and Color Technology, Amirkabir University of Technology, Tehran 15875-4413, Iran*
[2]*Color and Polymer Research Centre, Amirkabir University of Technology, Tehran 15875-4413, Iran*

(Received October 2, 2019; Revised March 2, 2020; Accepted April 16, 2020)

Abstract: In situ synthesis coating method of textile fabric is an efficient strategy to reduce the time and energies in comparison with ex situ synthesis methods. A facile in situ synthesis method was used to make TiO_2-Ag nanoparticles (NPs) coated fabric and compared with a traditional ex situ synthesis method by a photo-reduction approach. The effect of silver concentration was assessed for both methods. The corona discharge treatment was used to increase the adhesion of the coating to the surface of the fabric. The FESEM and map showed more even distribution of the TiO_2-Ag NPs coated fabric for in situ method in comparison with ex situ. DLS analysis was employed for determining the average particle size of the NPs colloids and show the fewer colloids average size of the in situ method than ex situ. The elemental analysis of the EDS and ICP showed a significant efficiency of the in situ synthesis method for silver nitrate reduction that leads to an increase in the nanoparticles concentration on the surface. Self-cleaning and antibacterial activity have been increased by in situ synthesis coating method in comparison with ex situ method. The enhancement of silver nitrate concentration led to a considerable increase in silver content for in situ method in comparison with ex situ method. However, the self-cleaning improvement showed a critical concentration at silver nitrate of 0.005 w/v%. The wash durability of the coated fabrics showed a significant increase in durability for in situ synthesis. The measurement of the mechanical strength of the fabrics showed no significant change with both methods of coating.

Keywords: In situ, Ex situ, Photoreduction, Ag-TiO_2 nanocomposite particles, Self-cleaning

Introduction

There are several noteworthy characteristics for photocatalysts such as self-cleaning, UV protection, anti-fungal and anti-bacterial activity [1,2]. Among the photocatalysts, titanium dioxide (TiO_2) is attractive due to the facile availability and high photocatalytic properties. The low bandgap of 3.2 eV of the TiO_2 provides a photochemical reaction to degrade the organic components by mineralization of the contaminants using photo-irradiation [3,4]. However, the high degree of recombination and low wavelength absorbance (in UV wavelength range) of the TiO_2 photocatalyst lead to a decrease in the efficiency of the photocatalytic properties [5-7]. There are several reports that demonstrate the improvement of the TiO_2 photocatalytic efficiency by noble metal ions doping [8-10]. The noble metal ions show a synergistic effect with TiO_2 NPs because of the existence of the plasmon resonance in silver nanoparticles and optical interactions [11]. The plasmon resonance of the silver extends the wavelength absorbance from UV rang to the visible range. In addition, the noble metals decrease the recombination rate of the TiO_2 NPs which results in increasing the electron-hole separation [12]. On the other hand, the TiO_2 nanoparticle is a good stabilizer for silver NPs colloids [13]. The silver metal ion is one of the most abundant noble metal elements that have been used as micro biocides and disinfectants [14-16]. There are critical concentrations of silver dopant for creating an optimized photocatalysis property on TiO_2/Ag NPs [17]. In the textile industry, the antibacterial finishing of cellulosic fibers is very noticed, because of their high tendency to thriving the microorganisms on a textile substrate. Therefore, many efforts were based on improving the antibacterial properties of cellulose fibers [18,19].

Adhesion phenomena are key criteria to increase the coating quality [20]. There are several surface modifications to increase the surface adhesion such as chemical, thermal, physical and plasma treatment [21]. Plasma treatment is a friendly environmental process that can modify the morphological and chemical characteristics of the surfaces without any change on the bulk properties [22] Several reports confirm the increase in the adhesion properties for different textile fabrics such as polyester [23-26], nylon [27, 28] and polypropylene [29]. Our previous study showed an increase in the hydrophilicity properties for polyester/ cellulose blended fabric by corona treatment [30].

The coating process is a usual method that induces a finishing for the textile fabrics [31]. Nowadays, the textile industry researchers are interested in a facile method to reduce the time, chemical material, water and energy consumption [32]. The in situ synthesis method is an efficient procedure to decrease the time and energy consumption. In this method, a textile fabric was immersed in an aqueous solution and the synthesis and coating

*Corresponding author: shahlashekarriz@aut.ac.ir

processes were treated simultaneously [33]. Therefore, it is necessary to compare the qualification of ex situ with in situ methods for finding the best efficient coating method for finishing the textile fabrics. Ex situ coating method has been performed by two main steps including the synthesis of the Ag/TiO_2 nanocomposite particles (NPs) and loading the nanoparticles on the fabric surface [34]. Likewise, there are several studies that reported the synthesis of Ag/TiO_2 NPs on the textile fabric substrates by in situ method. Allahyarzadeh *et al.* fabricated the Ag/TiO_2 NPs coated polyester fabric by an in situ chemical reduction method. The NaOH and CTAB were used as reducers [35]. Abid *et al.* used the same method with reverse steps for synthesizing Ag and TiO_2 NPs on the surface of cotton fabric [36]. Li *et al.* loaded the TiO_2 NPs on cotton fabric by hydrothermal treatment and then composed the Ag NPs by chemical reduction process with glucose and NaOH reducers [37]. Milosevic *et al.* immersed the polyester and polyester/cotton blended fabrics into TiO_2 dispersion and dried. In the next step, TiO_2 NPs coated fabrics were immersed in an $AgNO_3$ aqueous solution and the methyl alcohol, alanine and sun-light irradiation played roles as reducers for $AgNO_3$ precursor [38,39]. Our previous study showed a single step in situ synthesis method for loading $AgTiO_2$ NPs on polyester/cotton fabric. The photochemical reduction was used for Ag-TiO_2 NPs synthesis. The photochemical reduction method of silver precursors on TiO_2 nanoparticles has been attracted because of the facility and low chemical compound consumption [40].

This research focuses on the comparison of in situ with ex situ synthesis coating methods for polyester/cellulose fabric and also the effect of Ag concentration change on photocatalytic efficiency have been assessed. The corona discharge pretreatment was used to increase the adhesion properties of the P/C fabric surface. The Ag-doped TiO_2 NPs were synthesized by the photochemical reduction procedure. The effect of silver nitrate precursor on Ag NPs content was investigated for both methods of in situ and ex situ. The NPs distribution of coating was evaluated by FESEM and map analysis. The average size of the NPs colloids was investigated by DLS analysis. The EDS and ICP analyses were used to measure the quantification value of the coating elements. The self-cleaning, photocatalytic characteristics, antibacterial activity, wash durability and mechanical strength of the fabrics were assessed for both methods of in situ and ex situ coatings.

Experimental

Materials

A commercial bleached and mercerized polyester/cellulose blended fabric with a thread number of 81-255 was provided from Yazdbaf Company (Yazd, Iran) in which the cellulose fibers were contained cellulose and cotton fibers. The weft fibers were included by polyester of 100 % and the warp fibers included 74:26 polyester/cellulose blended fibers. The thickness of 0.2 mm and a density of 185 g/cm^2 were measured for the plain weave polyester/cellulose blended fabric. A commercial non-ionic detergent (RUCO 66670) was purchased from Rudolf Co. based on the fatty alcohol ethoxylated (Germany).

Preparation Method

The P/C fabrics were washed by 2 g/*l* aqueous solution of non-ionic detergent with liquor to goods ratio of 40:1, for 30 min at 60 ºC. The washed fabrics were rinsed and dried at the ambient temperature.

A commercial device (Naaj Corona, Naa Plastic Co., Tehran, Iran) was used to apply the corona discharge treatment with air gas at atmospheric pressure. A high voltage with 100 V was placed inside the nozzle jet and supplied a high-frequency pulse current power by the corona discharge generator. The washed P/C fabric was cut to square pieces with the dimensions of 20×20 cm^2 and placed on the silicon-coated backing roller holder and were rotated at 20 rpm rate. The distance between the backing roll and an aluminum electrode nozzle was adjusted to ~2 mm. The optimization process of the corona discharge treatment was reported in the previous study which assessed the effectiveness of the input power and exposure the time criteria [30]. Corona input power was adjusted to 800 W which was provided by an electric current of 8 A and voltage of 100 V and exposure time was 10 min.

Different concentrations of $AgNO_3$ aqueous solutions were prepared and stirred for 15 min. A TiO_2 NPs powder (1 %w/v) was gradually added to 100 m*l* $AgNO_3$ aqueous solution and sonicated in an ultrasonic bath for 30 min. The $AgNO_3/TiO_2$ suspension was stirred for 1 h in the dark to achieve the equilibrium adsorption between Ag ions and TiO_2 nanoparticles. For ex situ synthesis method, the $AgNO_3/TiO_2$ suspension was exposed under UVA irradiation for 1 h. The color of the suspension changed to brownish that showed the synthesis of Ag-TiO_2 NPs. The produced Ag-TiO_2 NPs powder was separated from the final suspension by centrifugation technique and rinsing. The Ag-TiO_2 NPs dispersion (1 %w/v) was provided by distilled water and Ag-TiO_2 NPs powder. The corona discharge pretreated P/C fabric was impregnated by Ag-TiO_2 dispersion and prepared by pad-dry-cure (padded with 70 % liquor pickup, dried at the ambient temperature, cured at 130 ºC for 5 min and 150 ºC for 3 min). For the in situ synthesis coating method, a facile procedure was used to create an Ag-TiO_2 NPs coated fabric that was reported in our previous study [40]. The corona pretreated fabric was immersed in the $AgNO_3/TiO_2$ suspension and then squeezed by padding mangle with 70 % liquor pickup and immediately exposed under UVA irradiation for 1 h. The UVA irradiation was provided by a UVA 100 W lamp. The mechanism of

Table 1. Preparation conditions of the P/C fabrics

Sample	Method	Corona discharge treatment		Ag-TiO_2 NPs coating	
		Input power	Exposure time	TiO_2 %	$AgNO_3$ %
S_0		-	-	-	-
S_1	Ex situ	-	-	1	0.005
S_2	In situ	-	-	1	0.005
S_3		800	10	-	-
S_4		800	10	1	0
S_5	Ex situ	800	10	1	0.005
S_6	Ex situ	800	10	1	0.1
S_7	In situ	800	10	1	0.0005
S_8	In situ	800	10	1	0.002
S_9	In situ	800	10	1	0.005
S_{10}	In situ	800	10	1	0.01
S_{11}	In situ	800	10	1	0.05
S_{12}	In situ	800	10	1	0.1

chemical reaction for synthesizing Ag-TiO_2 NPs was explained in our previous study [40]. The Ag-TiO_2 NPs coated fabric was cured at 130 ºC for 5 min and 150 ºC for 3 min. The color changes of the fabric to brownish confirmed the photo-reduction treatment after UVA exposure (the DRS spectra of Ag-TiO_2 coated fabrics by ex situ and in situ methods was shown in Figure S1, Supporting Information). Table 1 and diagram 1 show the preparation conditions of the P/C fabrics and the sample preparation process.

Characterization

The average particle size and morphological properties of the Ag-TiO_2 coated fabrics were depicted by A Mira 3-XMU field emission-scanning electron microscope (FESEM) that operated at 15 kV. Digimizer software was used to measure the average size of the nanoparticles. A gold sputter-coater (Bal-Tec) was used to coat a conductive layer on the surfaces of the fabrics. The FESEM was equipped with elemental analysis of Energy-dispersive X-ray spectroscopy (EDS, SAMX Company). The EDS detector investigates the content of the Ag and Ti elements for the coated fabrics. The map analysis provided the images of the distribution of the elements for the loaded Ag and Ti elements on the surface of the fabric.

The colloid size distribution of the Ag-TiO_2 NPs suspensions was evaluated by dynamic light scattering (DLS) in a model of Malvern Zetasizer Nano S (red badg-632.8 nm) (English). The Ag-TiO_2 suspension was directly tested after the sonicating step for the ex situ method. However, for preparing the Ag-TiO_2 suspension after the in situ synthesis coating method, the Ag-TiO_2 coated fabric was immersed in distilled water at the ambient temperature and then stirred for 2 h. The unabsorbed Ag-TiO_2 NPs were released in the distilled water and an Ag-TiO_2 NPs suspension was obtained. The obtained suspension was analyzed by DLS for the in situ synthesis method.

The silver weight content of the Ag-TiO_2 NPs coated fabrics were analyzed by inductively coupled plasma-optical emission spectrometry (ICP-OES; model: 730-ES, Varian). To prepare the proper liquid state of the sample, The Ag-TiO_2 NPs coated fabrics were solved in a nitric acid solution.

The color change of the coated fabric to brownish was investigated by diffuse reflectance spectroscopy (X-Rite Co., model: Color-Eye 7000, DRS) for the in situ synthesis coating method (The CIELAB color space and standard illuminant D64). The effect of Ag NPs concentration on optical characteristics was also investigated by DRS thereby reflectance and K/S values.

Self-cleaning characteristics of the Ag-TiO_2 NPs coated fabrics were evaluated by measuring the color changes of the methylene blue (0.005 w/v%) stains. A drop of the methylene blue aqueous solution was squeezed on the textile fabric and the stained fabrics were exposed under UVA (20 W), UVC (20 W) and sunlight irradiation for 24 h. To

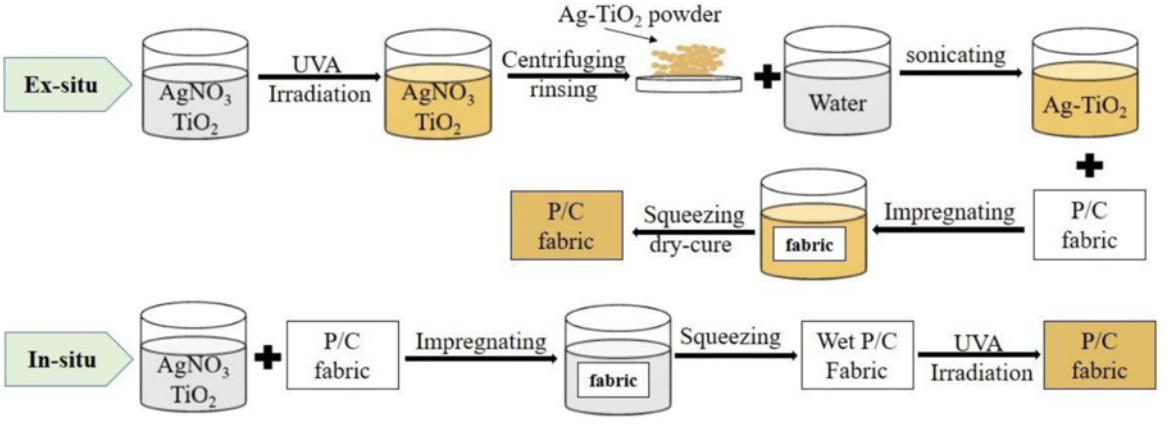

Figure 1. Diagram of preparation process for providing Ag-TiO_2 NPs coated fabrics by *in situ* and ex situ methods.

determine the color changes of the stain, DRS in the visible region utilized the ΔE values. The color changes in $L^*a^*b^*$ color space were calculated according to equation (1):

$$\Delta E^*_{ab} = \sqrt{(\Delta L^*)^2 + (\Delta a^*)^2 + (\Delta b^*)^2} \quad (1)$$

where L^*, a^*, and b^* are the lightness, green-red and blue-yellow indices, respectively.

Antibacterial Activity

The quantitative antibacterial activity was evaluated according to the standard of AATCC-100 for the coated fabrics. The circular swatches with a diameter of 4.8±0.1 cm were cut and sterilized in the autoclave. An untreated-uncoated fabric was used as the control swatch. The control and test swatches were inoculated with the test organisms. After incubation, the bacteria were evaluated from the swatches by shaking in known amounts of neutralizing solution. The number of bacteria present in this liquid was determined and the percentage reduction by the treated specimen was calculated. The *Escherichia coli* (*E. coli*) (ATCC 8379) and the *Staphylococcus aureus* (*S. aureus*) (ATCC 6538) were used as Gram-negative and Gram-positive bacteria, respectively. The percent reduction of bacteria by the specimen treatment by the following formulas is calculated (equation (2)):

$$R = 100 \times (B - A)/B \quad (2)$$

where R, A, and B are % reduction, the number of bacteria over the desired contact period (for 24 h) and the number of bacteria after inoculation (at 0 contact time), respectively.

Evaluation of Wash Durability

The wash durability standard of AATCC Test Method 61-2006 was used for the investigation of the Ag-TiO_2 coated fabrics (for both in situ and ex situ method). A laundering machine of Atlas Electric Device Launder-O-Meter (model: M/N LHDEF) was used to wash the Ag-TiO_2 coated fabrics at 40 ºC (time of 45 min) with non-ionic detergent. The washing process was run for five cycles such that each cycle is equal to 5, 10 and 15 cycles of commercial laundering. The EDS analysis shows the Ag and Ti element content of the samples after the washing process. The self-cleaning properties were also evaluated after the washing and drying process.

Mechanical Strength

The breaking force and elongation of P/C fabrics were measured by a tensile testing machine of SANTAM (model: STM-20 Cap. 20 kN, Iran) and a force was applied until the specimen breakage. The tensile strength test was performed according to the standard of ASTM D 5035-06. The specimens were cut to pieces of 25×150 mm^2 and a constant-time-to-break was adjusted at 20±3 s.

Results and Discussion

The reduction of water, chemical materials and energies has been noticed by the textile industry. The evaluation of the efficiency of the in situ method is an essential study to improve the finishing procedures of textile fabrics in comparison with ex situ method. For ex situ synthesis method, the Ag-TiO_2 NPs were created by photo-reduction and then coated by pad-dry-cure technique. For in situ method, the P/C fabric was impregnated by $AgNO_3$/TiO_2 aqueous solution and padded. After that, the wet fabric was exposed under UVA irradiation for the photo-reduction process and then cured. Therefore, the synthesis and coating methods were applied by a similar condition for both in situ and ex situ methods. The efficiency of the in situ and ex situ methods was compared by the assessment of characterization and applications of the Ag-TiO_2 coated P/C fabrics.

The effect of silver precursor ($AgNO_3$) on the optical characteristics of the Ag-TiO_2 NPs coated fabrics was investigated by DRS. The absorption spectra of Ag-TiO_2 coated fabrics were plotted in terms of the Kubelka-Munk (K/S) function. There is a characteristic peak of silver NPs due to creating a surface plasmon resonance (SPR) of silver NPs that is a function of absorption. There is no plasmon resonance for TiO_2 coated fabric whereas a plasmon resonance was observed for Ag-TiO_2 coated fabrics at the wavelength of 460 nm. After increasing the $AgNO_3$ concentration from 0.0005 to 0.1 %(w/v), the intensity of the plasmon peak increased that was attributed to the increase in Ag dopant concentration for the constant concentration of TiO_2 NPs. The absorption band was extended to higher wavelength with increasing Ag NPs doping such that the absorption edge of Ag-TiO_2 coated fabric with 0.1 %(w/v) (S_{12} sample) was shifted to <700 nm in comparison with TiO_2 coated fabric (S_4 sample) at 420 nm. This increase in absorption can be attributed to the surface plasmon resonance effect due to charge transfer between the TiO_2 NPs and Ag NPs.

In addition to the usual properties, the aesthetic appearance of the fabrics is essential to estimate the customer's expectations. The color change of the fabric from white to the shades of brown leads to a decrease in the attractive appearance of the fabrics. Therefore, it is necessary to preserve the initial whiteness of the fabrics. An increase in Ag dopant concentration leads to change the color from white to shades of brown. The color change of ΔE^*_{ab} was measured by DRS in $L^*a^*b^*$ color space for different concentrations of $AgNO_3$ precursor which were used for in situ synthesis coating method (Table 2). The blank fabric (S_0 sample) was used as the control sample with the initial Lab and the ΔE^*_{ab} was estimated for S_4, S_7, S_8, S_9, S_{10}, S_{11} and S_{12} samples according to equation (1). The ΔE^*_{ab} was increased

Table 2. Color change of ΔE^*_{ab} for S_4, S_7, S_8, S_9, S_{10}, S_{11}, and S_{12} samples

Sample	ΔE^*_{ab}
S_4	0.66
S_7	0.18
S_8	0.70
S_9	1.08
S_{10}	6.22
S_{11}	40.25
S_{12}	48.77

by increasing the concentration of Ag NPs dopant. S_7, S_8 and S_9 samples showed an acceptable ΔE^*_{ab} and preserved the initial appearance of the fabrics.

Morphological Properties and Map Analysis

The morphological properties of the corona discharge pre-treatment and Ag-TiO_2 coating treatment can be depicted by FESEM images. The FESEM images of the blank fabric (S_0 sample), corona pretreated fabric (S_3 sample), corona pretreated-coated fabric by ex situ method (S_5 sample) and corona pretreated-coated fabric by in situ method (S_9 sample) were shown in Figure 2a-h. The blank fabric (S_0 sample) showed a relatively smooth surface (Figures 2a and 2b). The morphological characteristic of the surface was changed significantly after corona discharge treatment (for the S_3 sample) so that a rough surface was shown due to the etching approach (Figures 2c and 2d). The reactive species of corona discharge treatment bombard the polymer chains and lead to happening the chain scission. The chain scission causes the degradation of polymer chains and creating several pores and cavities on the surface of the fabric. The created pores and cavities on the P/C surface provided sufficient sites for embedding the Ag-TiO_2 NPs coating. The increase in surface roughness improves the Ag-TiO_2 coating process that have been confirmed by several studies [41-43]. As depicted in Figure 2e-h, in most cases, the Ag-TiO_2 NPs were placed into the cavities and pores. The ex situ synthesis coating method (S_5 sample) showed uneven nanoparticles loading while the in situ synthesis coating method (S_9 sample) showed more evenly nanoparticles loading on the surface of the fabric. Therefore, it was expected more uniform self-cleaning, photocatalytic and antibacterial properties for in situ method. Likewise, the in situ coated sample showed more Ag-TiO_2 NPs contents in comparison with ex situ coated sample that leads to improving the efficiency of the multifunctional finished fabric. The average sizes of 36±5 nm for the S_5 sample and 27±5 nm for the S_9 sample were measured by Digimizer software. The smaller average size of the Ag-TiO_2 NPs composites for in situ synthesis method can be attributed to the higher control of the nucleation and growth of Ag NPs on the fabric surface because the in situ

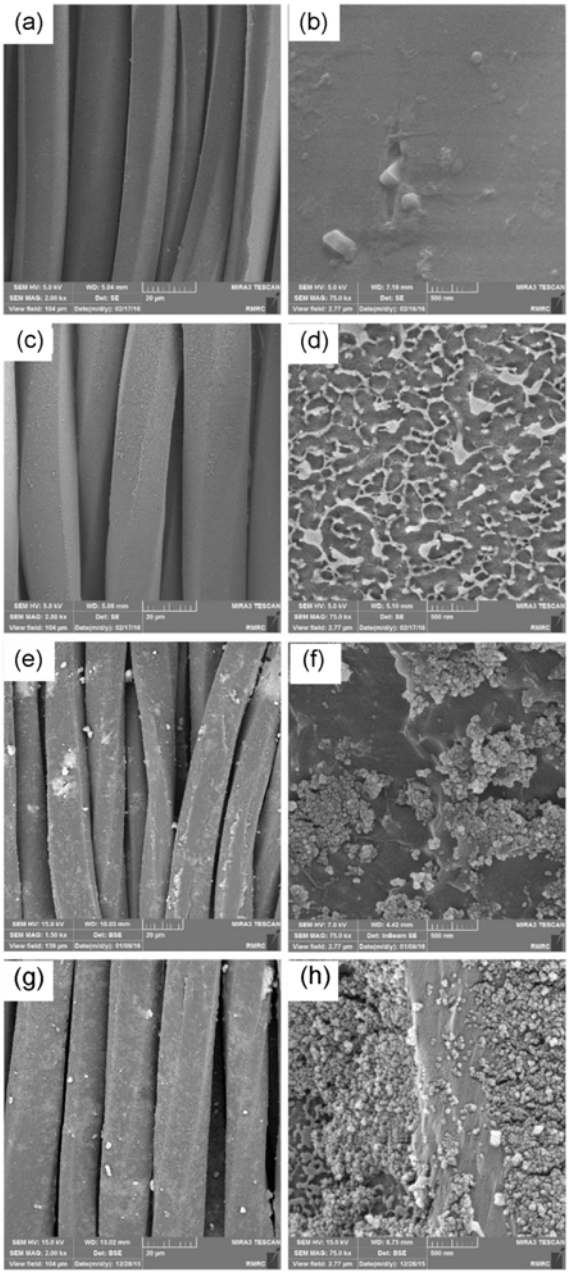

Figure 2. FESEM images for S_0 (a and b), S_3 (c and d), S_5 (e and f), and S_9 (g and h) with magnification of 2000 and 75000.

method provides a substrate (fabric) for the deposition and fixation of the TiO_2 NPs before beginning the synthesis process. Therefore, there are many fixed nucleus of TiO_2 NPs for growing Ag NPs for in situ method. For ex situ method, there is an unstable dispersion that was unevenly irradiated by UVA because the irradiation was less received in the depth of the dispersion container. Therefore, the more stability of the dispersion for in situ method leads to the decrease in the size distribution of the NPs composite and an increase in the evenness of NPs composite loading. It can be

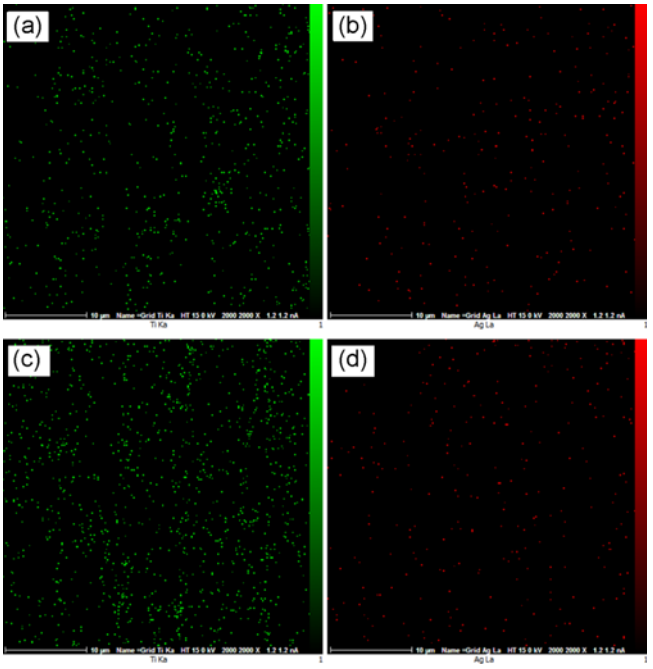

Figure 3. Map analysis of S_5 (a and b) and S_9 (c and d); red: Ag element, and green: Ti element.

confirmed that the in situ synthesis coating method provides more efficient condition to create a high quality multifunctional finished fabric and reduces the wastewater exhaustion, water, chemical material and energies consumption.

Figure 3a-d presents the density and distribution of the Ag-TiO_2 NPs in the surface of the P/C fabric by the map analysis. The Ti and Ag elements showed more even distributions and higher NPs density for in situ method in comparison with ex situ synthesis coating method.

DLS Analysis

The DLS analysis presents the average size of stabled particles in Ag-TiO_2 dispersion. The balance between attractive and repulsive forces of particles leads to create a stable dispersion for nanoparticles which was confirmed by DLVO Theory. A stable dispersion shows a zeta potential with lower than -25 mV and higher than +25 mV, which shows the electric stability of the particles. The zeta potential of 47.5±6.75 and 49.54±6.42 was recorded for Ag-TiO_2 NPs dispersion of ex situ method and Ag-TiO_2 NPs dispersion of in situ method, respectively that confirm more stability of the Ag-TiO_2 NPs dispersion of in situ method than Ag-TiO_2 NPs dispersion of ex situ method. A stable dispersion provides an important role in the uniform size distribution of NPs on the fabric surface. Subsequently, it can be expected that the Ag-TiO_2 NPs dispersion of in situ method provides fewer size distribution for Ag-TiO_2 NPs coated fabric. Figure 4 shows the size distribution of Ag-TiO_2 NPs which was evaluated for the dispersion including Ag-TiO_2 NPs

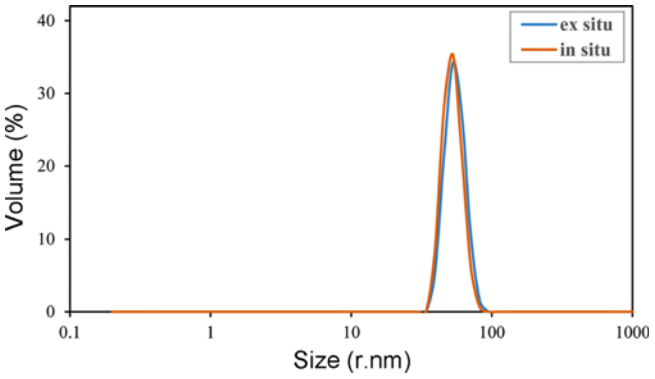

Figure 4. DLS analysis of the Ag-TiO_2 NPs coated fabrics by ex situ and in situ methods.

(synthesized by ex situ and in situ methods). The average particle sizes of the colloids were 55.21 and 52.81 r.nm for Ag-TiO_2 NPs dispersion of ex situ and in situ method, respectively. Therefore, the in situ synthesis method decreased the average particle size of the Ag-TiO_2 NPs for coated fabric which confirms the obtained values to those measured by FESEM.

EDS Analysis

The elemental analysis of the blank fabric (S_0 sample), corona pretreated fabric (S_3 sample), corona pretreated-coated fabric by ex situ method (S_5 and S_6 samples) and corona pretreated-coated fabric by in situ method (S_9 and S_{12} samples) was estimated by the quantitative elemental analysis of EDS which measures the content of C, O, N, Ti and Ag elements on the surface of the P/C fabric (Figure 5a-d). The weight percentage of the oxygen elements is increased after corona discharge treatment for the S_3 sample (Figure 5b) due to the functionalization of the P/C fabric by oxygen-containing activated groups of air corona discharge treatment. Likewise, the nitrogen element was created after corona discharge treatment that is attributed to the interaction of the P/C fabric with nitrogen-containing activated groups.

A significant increase in Ag element weight percentage for in situ coated fabrics for both $AgNO_3$ concentrations of 0.005 and 0.1 %(w/v) (0.29 and 2.54 %W, respectively) in comparison with ex situ coated fabric can be observed (0.12 and 0.14 W%, respectively). The enhancement of $AgNO_3$ concentration from 0.005 to 0.1 %(w/v) leads to an increase in the Ag NPs dopant on coated fabric for both in situ and ex situ methods. However, the weight percentage of Ag elements of the in situ coated fabric with 0.1 %(w/v) (S_{12} sample) showed a significant increase with increasing $AgNO_3$ concentration. In conclusion, the loading Ag-TiO_2 NPs on the surface of the in situ synthesis method is more efficient in comparison with ex situ synthesis method.

For in situ synthesis coating method, the fabric was floated in TiO_2/$AgNO_3$ dispersion and then squeezed. In this step,

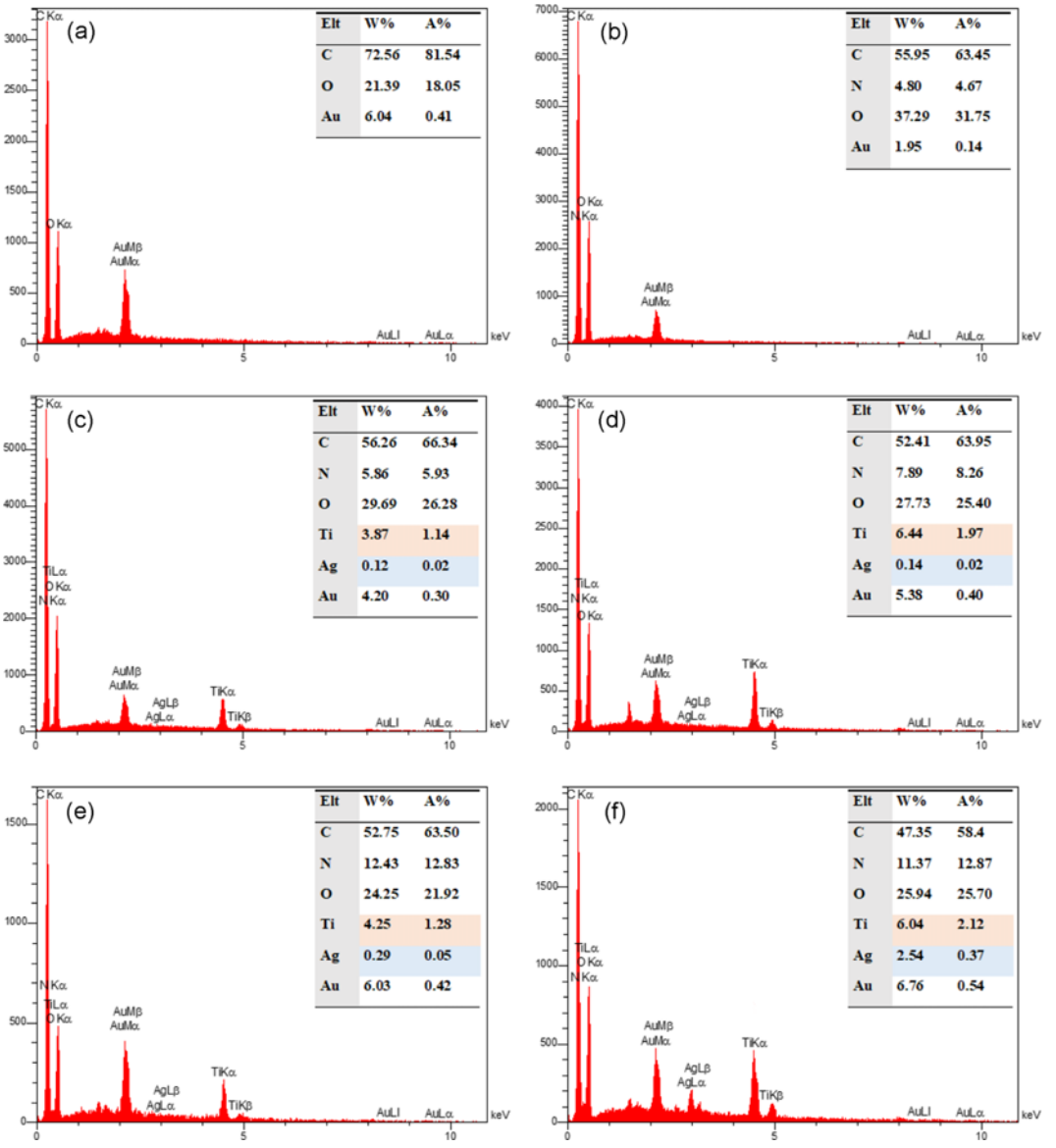

Figure 5. EDS analysis of the (a) S_0, (b) S_3, (c) S_5, and (d) S_6 (e) S_9 (f) S_{12} samples.

the TiO_2 NPs were loaded on wet impregnated fabric and placed on susceptible sites of the fabric surface. Consequently, there is an appropriate substrate for nucleation and growth of Ag NPs such that each TiO_2 NPs plays the nucleus role. For ex situ method, the $TiO_2/AgNO_3$ dispersion is unstable that leads to the agglomeration of TiO_2 NPs and a decrease in the nucleus. The less addition of Ag NPs dopant for ex situ method with increasing the $AgNO_3$ concentration from 0.005 to 0.1 %(w/v) can be attributed to a decrease in the amount of nucleus which is due to the instability and agglomeration of dispersion. Furthermore, the hydroxyl functional groups of cellulose (for in situ method) operate as a weak chemical reducing agent that leads to the synthesis of the Ag NPs. Therefore, the hydroxyl functional groups can be applied as the nucleation sites.

ICP Analysis

The EDS results showed a significant increase in Ag NPs weight percentage with increasing $AgNO_3$ concentration to 0.1 %(w/v). To confirm this increase, ICP analysis was used. The ICP is a quantitative ideal tool for measuring the concentration of the NPs in aqueous solutions due to its unique ability for rapid detection of the elements and high sensitivity. ICP was used to estimate the concentration of Ag NPs dopant for S_6 and S_{12} samples which are loaded on the TiO_2 NPs. It was observed that Ag concentration of 18.351 ppm for in situ synthesis coated fabric (S_{12}) that showed a significant increase in comparison with ex situ synthesis

coated fabric (S_6) with an Ag concentration of 0.114 ppm.

Self-cleaning and Wash Durability

The self-cleaning properties of S_0, S_1, S_2, S_3, S_4, S_5, S_7, S_8, S_9 and S_{10} samples were investigated by measuring the discoloration of the color stain of methylene blue after exposing UVA, UVC and daylight irradiation for 24 h (Table 3). The increase in the $AgNO_3$ concentration from 0.005 to 0.01 %(w/v) (S_7 to S_{12} samples) leads to improve the self-cleaning properties which were arisen for in situ coating process. A twofold concentration of $AgNO_3$ aqueous solution for S_{10} sample in comparison with S_9 sample confirms that the 0.005 %(w/v) is the critical concentration for obtaining the optimum self-cleaning properties for in situ synthesis coating. The in situ coated fabrics showed superior self-cleaning in comparison with ex situ coated fabrics for both untreated and corona discharge pretreated fabrics. Corona discharge pretreatment improved the self-cleaning properties due to increasing the adhesion of the fabric surface. Subsequently, the corona pretreated and in situ synthesis methods provide efficient conditions to improve the self-cleaning properties of Ag-TiO_2 coated fabrics.

The effect of the washing process on self-cleaning properties of the Ag-TiO_2 coated fabrics was evaluated for S_5 and S_9 samples after 5, 10 and 15 cycles of laundering process (Table 4). Both S_5 and S_9 samples showed a decrease in the methylene blue discoloration. Nevertheless, the in situ coated fabric (S_9 sample) showed less decrease in comparison with ex situ coated fabric (S_5 sample). Therefore, the in situ synthesis method was more efficient in self-cleaning durability properties than ex situ method.

The EDS analysis of Ag-TiO_2 NPs coated fabric for both in situ and ex situ synthesis methods was estimated after the washing process (Figure 6) which was compared by Figure 5 (e and f). After the washing process, the content of Ag and Ti elements showed more NPs composite concentrations for the in situ synthesis coating method than the ex situ method. Consequently, the EDS results showed more wash durability for the in situ synthesis method. The enhancement of the NPs concentration for in situ method was due to increasing the chemical interactions with more intensity between Ag-TiO_2 NPs and cellulosic and polyester structures which were confirmed in the previous study [40]. The hydroxyl groups of the cellulose structure can also play a role of weak reduction due to the existence of hydroxyl groups [35]. However, there are weak interactions between NPs and the fabric surfaces for the ex situ synthesis method.

Antibacterial Activity

The antibacterial activity of the S_0, S_1, S_2, S_3, S_5 and S_9 samples were estimated by the quantitative test method of

Table 3. Self-cleaning results of the Ag-TiO_2 coated fabrics by measuring the discoloration of methylene blue stain after 24 h irradiation under UVA, UVC, and daylight

Sample	ΔE after 24 h irradiation		
	UVA	UVC	Daylight
S_0	13.98	12.76	15.15
S_1	37.90	34.60	42.62
S_2	43.58	39.25	52.73
S_3	14.32	13.40	16.59
S_4	39.76	35.13	44.31
S_5	39.87	35.98	47.2
S_7	42.65	37.87	49.66
S_8	45.7	39.75	55.75
S_9	47.04	45.33	60.49
S_{10}	49.32	46.63	61.47

Table 4. Wash durability results of the Ag-TiO_2 coated fabrics by measuring the discoloration of methylene blue stain after 24 h irradiation under daylight

Sample	ΔE after 24 h irradiation			
	Before washing	After 5 cycle	After 10 cycle	After 15 cycle
S_5	47.2	38.43	31.3	25.6
S_9	60.49	57.61	53.18	47.83

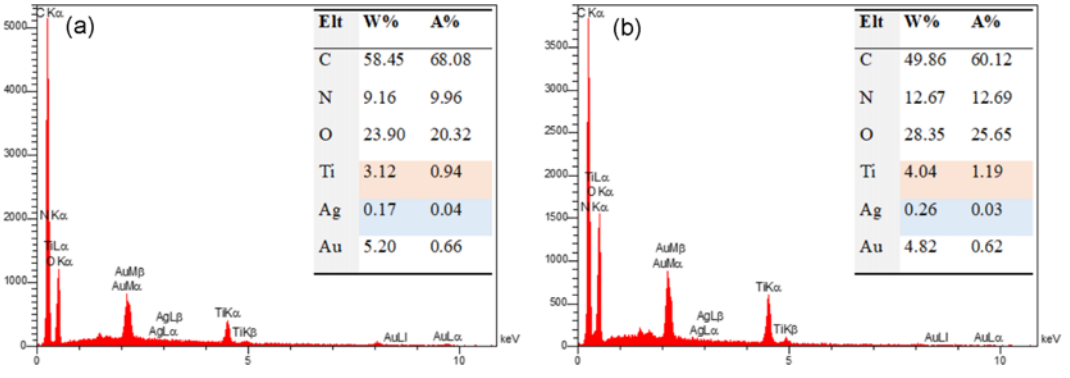

Figure 6. EDS analysis of the Ag-TiO_2 coated fabrics for (a) washed S_5 sample and (b) washed S_9 sample.

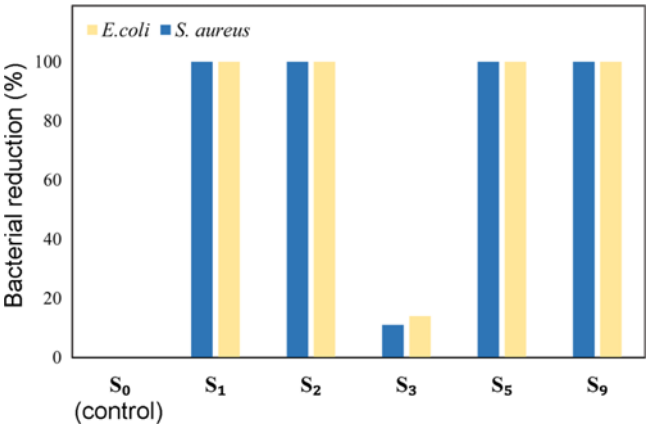

Figure 7. Antibacterial activity of Ag-TiO_2 NPs coated fabric for both *E. coli* and *S. aureus* bacteria.

AATCC-100 (Figure 7). The blank P/C fabric (S_0 sample) was used as the control swatch and shows no antibacterial activity. The S_1, S_2, S_5 and S_9 samples showed 100 % antibacterial activity for both *E. coli* and *S. aureus* bacteria. Therefore, the effect of corona discharge pretreatment and the Ag-TiO_2 synthesis method on the antibacterial is negligible. Meanwhile, the corona pretreated fabric (sample S_3) showed a little antibacterial due to the presence of several functional groups such as carboxylic, alcohols and amines. These functional groups are biologically active [44, 45].

Mechanical Strength

The breaking force and elongation data of the samples were collected in Table 5. The elongation data after corona discharge pretreatment showed a decrease while the coating process did not present any sensible changes for warp and weft fibers. The breaking force of warp showed no significant changes after the corona pretreatment and coating process. However, a clear increase in breaking force of weft fibers can be observed after the coating process while the corona pretreatment presented no sensible changes. Therefore, the corona pretreatment faintly decreases the elongation of the warp fibers. The coating process is ineffective on the mechanical strength of the coated fabrics and even increases the mechanical strength in some cases (weft fibers of S_1, S_2, S_5 and S_9 samples).

Table 5. Mechanical strength of the in situ and ex situ Ag-TiO_2 NPs coated samples before and after corona pretreatment

Sample	Elongation data (mm)		Breaking force (N)	
	Warp	Weft	Warp	Weft
S_0	24.17	31.06	313.13	234.95
S_1	24.15	30.18	313.01	243.76
S_2	24.17	32.45	311.43	248.50
S_3	21.34	28.77	313.90	235.13
S_5	21.16	28.98	313.09	243.87
S_9	21.70	29.59	315.57	258.73

Conclusion

A comparative study was presented for creating an Ag-TiO_2 coated P/C fabric using two synthesis methods of in situ and ex situ. The corona pretreatment was applied to increase the adhesion properties of the fabric surface. The morphological properties of P/C fabrics showed an increase in the roughness after corona pretreatment. Likewise, the average sizes of 36±5 nm for ex situ coated sample and 27±5 nm for in situ coated sample were obtained. Both FESM and map analysis showed more even distributions of NPs on the fabric surface for in situ method. DLS showed a stable dispersion with average particle sizes of 55.21 and 52.81 r.nm for ex situ and in situ synthesis methods, respectively. The EDS and ICP analysis confirmed the increase in the Ag-TiO_2 NPs concentration for in situ method in comparison with ex situ method. The in situ coated fabric showed an efficient self-cleaning fabric with excellent antibacterial activity and wash durability. The changes in the mechanical strength were also negligible after the corona pretreatment and coating process.

Electronic Supplementary Material (ESM) The online version of this article (doi: 10.1007/s12221-021-9049-6) contains supplementary material, which is available to authorized users.

References

1. Y. Huang, S. S. H. Ho, Y. Lu, R. Niu, L. Xu, J. Cao, and S. Lee, *Molecules*, **21**, 56 (2016).
2. M. E. El-Naggar, T. I. Shaheen, S. Zaghloul, M. H. El-Rafie, and A. Hebeish, *Ind. Eng. Chem. Res.*, **55**, 2661 (2016).
3. J. Schneider, M. Matsuoka, M. Takeuchi, J. Zhang, Y. Horiuchi, M. Anpo, and D. W. Bahnemann, *Chem. Rev.*, **114**, 9919 (2014).
4. G. Jiang, Z. Lin, C. Chen, L. Zhu, Q. Chang, N. Wang, W. Wei, and H. Tang, *Carbon*, **49**, 2693 (2011).
5. H. Li, G. Zhao, Z. Chen, B. Song, and G. Han, *J. Am. Ceram. Soc.*, **93**, 445 (2010).
6. R. Daghrir, P. Drogui, and D. Robert, *Ind. Eng. Chem. Res.*, **52**, 3581 (2013).
7. S. G. Kumar and L. G. Devi, *J. Phys. Chem. A*, **115**, 13211 (2011).
8. S. F. Chen, J. P. Li, K. Qian, W. P. Xu, Y. Lu, W. X. Huang, and S. H. Yu, *Nano Res.*, **3**, 244 (2010).
9. J. He, I. Ichinose, T. Kunitake, and A. Nakao, *Langmuir*, **18**, 10005 (2002).

10. A. G. Hassabo, M. E. El-Naggar, A. L. Mohamed, and A. A. Hebeish, *Carbohyd. Polym.*, **210**, 144 (2019).
11. G. Cacciato, M. Bayle, A. Pugliara, C. Bonafos, M. Zimbone, V. Privitera, M. G. Grimaldi, and R. Carles, *Nanoscale*, **7**, 13468 (2015).
12. V. Rodríguez-González, S. O. Alfaro, L. Torres-Martínez, S.-H. Cho, and S.-W. Lee, *Appl. Catal. B.*, **98**, 229 (2010).
13. P. D. Cozzoli, R. Comparelli, E. Fanizza, M. L. Curri, A. Agostiano, and D. Laub, *J. Am. Chem. Soc.*, **126**, 3868 (2004).
14. M. Banach, L. Tymczyna, A. Chmielowiec-Korzeniowska, and J. Pulit-Prociak, *Bioinorg. Chem. Appl.*, **2016**, 1 (2016).
15. M. E. El-Naggar, S. Shaarawy, and A. A. Hebeish, *Int. J. Biol. Macromol.*, **106**, 1192 (2018).
16. J. Yan, A. M. Abdelgawad, M. E. El-Naggar, and O. J. Rojas, *Carbohyd. Polym.*, **147**, 500 (2016).
17. Y. Cao, H. Tan, T. Shi, T. Tang, and J. Li, *J. Chem. Technol. Biot*., **83**, 546 (2008).
18. M. Rehan, M. E. El-Naggar, H. M. Mashaly, and R. Wilken, *Carbohyd. Polym.*, **182**, 29 (2018).
19. A. L. Mohamed, M. E. El-Naggar, T. I. Shaheen, and A. G. Hassabo, *Microsyst. Technol.*, **22**, 979 (2016).
20. Z. Chen, K. Zhou, X. Lu, and Y. C. Lam, *Acta Mech.*, **225**, 431 (2014).
21. T. Govindarajan and R. Shandas, *Polymers*, **6**, 2309 (2014).
22. E. Liston, L. Martinu, and M. Wertheimer, *J. Adhes. Sci. Technol.*, **7**, 1091 (1993).
23. C. Wang, Y. Liu, H. Xu, Y. Ren, and Y. Qiu, *Appl. Surf. Sci.*, **254**, 2499
24. K. Gotoh and S. Yoshitaka, *Text. Res. J.*, **83**, 1606 (2013).
25. C. Zhang, M. Zhao, L. Wang, L. Qu, and Y. Men, *Appl. Surf. Sci.*, **400**, 304 (2017).
26. K. Fang and C. Zhang, *Appl. Surf. Sci.*, **255**, 7561 (2009).
27. G. Wade and W. Cantwell, *J. Mater. Sci. Lett.*, **19**, 1829 (2000).
28. F. Emami, S. Shekarriz, Z. Shariatinia, and Z. M. Mahdieh, *Fiber. Polym*., **19**, 1014 (2018).
29. S. Shahidi and M. Ghoranneviss, *Fiber. Polym.*, **13**, 971 (2012).
30. Z. M. Mahdieh, S. Shekarriz, F. A. Taromi, and M. Montazer, *Carbohyd. Polym*., **198**, 17 (2018).
31. K. Singha, *Am. J. Polym. Sci.*, **2**, 39 (2012).
32. A. Hasanbeigi and L. Price, *Renew. Sust. Energ. Rev.*, **16**, 3648 (2012).
33. S. Mowafi, M. Rehan, H. M. Mashaly, A. A. El-Kheir, and H. E. Emam, *J. Text. I.*, **108**, 1828 (2017).
34. M. Montazer and M. M. Amiri, *J. Phys. Chem. B*., **118**, 1453 (2014).
35. V. Allahyarzadeh, M. Montazer, N. H. Nejad, and N. Samadi, *J. Appl. Polym. Sci.*, **129**, 892 (2013).
36. M. Abid, S. Bouattour, A. M. Ferraria, D. S. Conceição, A. P. Carapeto, L. F. V. Ferreira, A. M. B. do Rego, M. M. Chehimi, M. R. Vilar, and S. Boufi, *J. Colloid Interface Sci.*, **507**, 83 (2017).
37. S. Li, T. Zhu, J. Huang, Q. Guo, G. Chen, and Y. Lai, *Int. J. Nanomedicine*, **12**, 2593 (2017).
38. M. Milošević, M. Radoičić, Z. Šaponjić, T. Nunney, D. Marković, J. Nedeljković, and M. Radetić, *J. Mater. Sci*., **48**, 5447 (2013).
39. M. Milošević, M. Radoičić, Z. Šaponjić, T. Nunney, C. Deeks, V. Lazić, M. Mitrić, T. Radetić, and M. Radetić, *Cellulose*, **21**, 3781 (2014).
40. Z. M. Mahdieh, S. Shekarriz, F. A. Taromi, and M. Montazer, *Cellulose*, **25**, 2355 (2018).
41. J. P. Fernández-Blázquez, D. Fell, E. Bonaccurso, and A. Del Campo, *J. Colloid Interface Sci.*, **357**, 234 (2011).
42. S. Inbakumar, R. Morent, N. De Geyter, T. Desmet, A. Anukaliani, P. Dubruel, and C. Leys, *Cellulose*, **17**, 417 (2010).
43. H. Dave, L. Ledwani, N. Chandwani, N. Chauhan, and S. Nema, *J. Text. I.*, **105**, 586 (2014).
44. C. E. Duru, I. A. Duru, F. C. Ibe, I. O. Achinihu, and L. Ukiwe, *IOSR-JAC*, **8**, 35 (2015).
45. M. Moovendhan, P. Seedevi, A. Shanmugam, and V. Shanmugam, *J. Biol. Act. Prod. Nat.*, **5**, 52 (2015).